DOI:10.31557/APJCC.2026.11.6.803

RESEARCH ARTICLE

Breast Cancer–Targeted Doxorubicin Therapy via Folate-Conjugated Nanoliposomal Carriers

Tabassom Mahmoudie[1], Meysam Ebrahimifar[2], Mehrshad Fekri[3], Mozhgan Dahmardnezhad[4], Fatemeh Jamshidi[5], Fattakhov Ravshan Abdurashidovich[6], Yunuskhodjaeva Madina Kamalitdinovna[7], Khamidova Dilbar Avdunovna[8], Khatypova Marvara Garifovna[8], Khadjimetov Abdurasul Abdugafurovich[9], Narova Nargiza Elbekovna[10], Yunuskhanova Kamila Shavkatovna[11], Lola Akhmedova[12], Yokudkhon Alimullaeva[13], Nargiza Kamilova[14], Ruzieva Zebo Ibodilloevna[15], Mohammadreza Allahyartorkaman[16]*

[1]Faculty of Pharmacy, Tabriz University of Medical Sciences, Tabriz, Iran. [2]Department of Toxicology, Faculty of Pharmacy, Islamic Azad University, Shahreza Branch, Shahreza, Iran. [3]Department of Biochemistry, NT.C., Islamic Azad University, Tehran, Iran. [4]School of Medicine, Arak University of Medical Sciences, Arak, Iran. [5]Quality Control Department, Anzan Teb Azma, Tehran, Iran. [6]DSc, Associate Professor of the Alfraganus University, Tashkent, Uzbekistan. [7]DSc, Associate Professor of the Department of Preventive Dentistry, Tashkent State Medical University , Tashkent, Uzbekistan. [8]PhD, Associate Professor of the Postgraduate Medical Education Faculty, Tashkent State Medical University, Tashkent, Uzbekistan. [9]PhD, Associate Professor of the Postgraduate Medical Education Faculty, Tashkent State Medical University, Tashkent, Uzbekistan. [10]DSc, Associate Professor of the Alfraganus university, Tashkent, Uzbekistan. [11]PhD, Assistant, Department of Advanced Training in Therapeutic Dentistry with a Course in Orthopedic Dentistry, Tashkent State Medical University, Tashkent, Uzbekistan. [12]PhD, Assistant, Department of Advanced Training for Mid-Level Medical Personnel, Tashkent State Medical University, Tashkent, Uzbekistan. [13]Head of the Department of Advanced Training of Medical Workers with Secondary Education,Tashkent State Medical University, Tashkent, Uzbekistan. [14]PhD, Assistant, Head of the Department of Advanced Training of Medical Workers with Secondary Education, Tashkent State Medical University, Tashkent, Uzbekistan. [15]Department of Advanced Medical Training, Tashkent State Medical University, Tashkent, Uzbekistan. [16]Regional Tuberculosis Reference Laboratory, Tehran University of Medical Sciences, Tehran, Iran.

Abstract

Introduction: Targeted drug delivery systems have emerged as a promising strategy to enhance therapeutic efficacy and minimize off-target toxicity in cancer therapy. In this study, folic acid–conjugated nanoliposomes (FA-NLs) were developed as a selective delivery vehicle for doxorubicin (DOX) to folate receptor–overexpressing breast cancer cells (MCF-7). **Materials and Methods:** FA-NLs were synthesized using the thin-film hydration method and loaded with DOX. The nanocarriers were characterized by SEM, TEM, and DLS to determine morphology, size distribution, and zeta potential. Drug encapsulation efficiency (EE%) and in vitro release profiles at physiological and acidic pH were assessed. Cytotoxicity was evaluated via MTT assay in MCF-7 cells. Cellular uptake was analyzed using fluorescence microscopy. Apoptosis induction was quantified through Annexin V/PI flow cytometry. **Results:** FA-NLs exhibited uniform spherical morphology with a mean particle size of 182 nm (PDI: 0.24) and a negative surface charge (−34 mV). The formulation achieved high DOX encapsulation (EE%: 92%) with drug loading of 2 %, and demonstrated pH-responsive sustained release over 50 h (~90% at pH 5.2 vs ~62% at pH 7.4). In MCF-7 cells, FA-NLs enhanced anticancer activity relative to non-targeted liposomes and free DOX, with the IC_{50} decreasing from ~20 μM (free DOX; F5) to ~7 μM (FA/FL-DOX; folate-depleted; F1) (≈2.9-fold reduction). Flow cytometry confirmed stronger apoptosis induction, including higher late apoptosis compared with conventional DOX. **Conclusion:** These results demonstrate the strong potential of FA-NLs as a smart nanocarrier system to enhance intracellular uptake and apoptosis-mediated anticancer efficacy of DOX in folate receptor–positive breast cancer cells, supporting further translational evaluation for precision oncology.

Keywords: Nanoliposome- Folic acid- Targeted drug delivery- Breast cancer- Doxorubicin

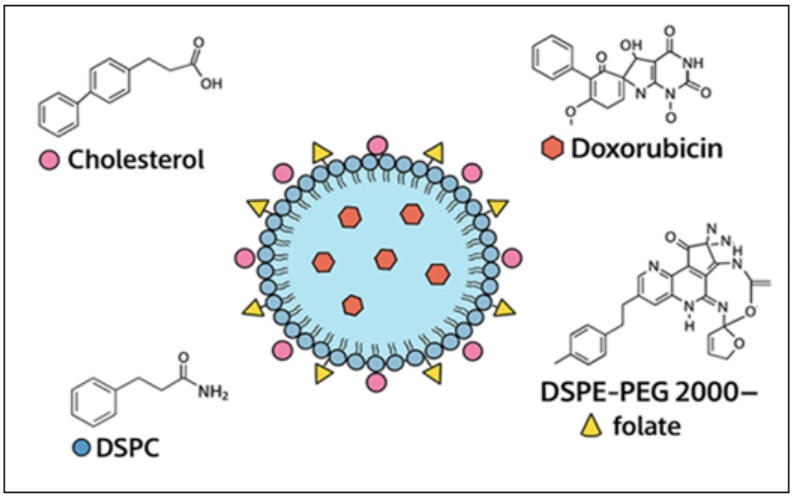
Asian Pac J Cancer Care, **11 (6)**, 803-812

Submission Date: 07/06/2026 Acceptance Date: 09/01/2026

Corresponding Author:
Dr. Mohammadreza Allahyartorkaman
Regional Tuberculosis Reference Laboratory, Tehran University of Medical Sciences, Tehran, Iran.
Email: Mohammad@as.edu.tw

Introduction

Breast cancer remains one of the most prevalent and deadly malignancies affecting women worldwide, accounting for a significant proportion of cancer-related morbidity and mortality [1, 2]. Although conventional chemotherapy has improved survival outcomes, its clinical efficacy is often limited by poor tumor selectivity, systemic toxicity, and multidrug resistance [3]. These challenges highlight the urgent need for advanced drug delivery systems that can enhance the specificity and therapeutic index of chemotherapeutic agents [4]. Nanotechnology-based drug delivery platforms have gained considerable attention in recent years due to their ability to improve pharmacokinetics, protect drugs from premature degradation, and facilitate targeted delivery to tumor tissues [5-8]. In other words, nanoscale vesicles carry a diverse repertoire of functional biomolecules that enable targeted interactions with host immune cells, cellular signaling pathways, cancer cells, and other biological targets [9, 10]. For instance, nanoparticles can be used for targeted drug delivery and cancer research, enabling tumor-specific targeting that minimizes off-target side effects and enhances antitumor efficacy [11]. Among these platforms, nanoliposomes spherical vesicles composed of lipid bilayers have emerged as biocompatible carriers capable of encapsulating both hydrophilic and hydrophobic drugs [12]. However, passive accumulation of liposomes via the enhanced permeability and retention (EPR) effect alone is insufficient for effective drug delivery, particularly in heterogeneous tumors such as breast cancer [13]. To overcome this limitation, active targeting strategies have been developed by modifying liposomal surfaces with ligands that selectively bind to overexpressed receptors on cancer cells [14]. One such receptor is the folate receptor alpha (FRα), which is highly expressed in various cancers including breast, ovarian, and lung cancers, but exhibits limited expression in most normal tissues [14, 15]. Folic acid (FA), a small and stable molecule with strong affinity for FRα, has been widely used as a targeting ligand to improve selective uptake of nanocarriers via receptor-mediated endocytosis [16]. Doxorubicin (DOX) is one of the most potent and widely used chemotherapeutic drugs for the treatment of breast cancer [17]. However, its clinical application is severely restricted by dose-dependent cardiotoxicity and non-specific tissue distribution [18, 19]. Encapsulation of doxorubicin in folic acid-conjugated nanoliposomes offers a promising approach to improve its tumor specificity, reduce systemic toxicity, and enhance therapeutic efficacy [19, 20]. So, humankind has always strived to overcome therapeutic challenges, continually refining and integrating medical methods and treatment approaches to achieve effective and acceptable solutions for patient care [21, 22]. Although folate-targeted liposomes have been widely investigated for breast cancer drug delivery, a recurring limitation in the literature is that many studies remain largely formulation-descriptive and do not rigorously demonstrate that enhanced anticancer effects are specifically driven by folate receptor (FR) engagement rather than nonspecific liposomal uptake [14-16]. In addition, mechanistic validation is often restricted to viability outcomes, while competitive folate blocking and quantitative apoptosis profiling are underused [16]. As a result, the true contribution of receptor-mediated targeting and its downstream cell-death consequences remains insufficiently resolved in many FA-liposome reports. In this study, we developed doxorubicin-loaded folic acid–conjugated nanoliposomes (FA-NLs) using a straightforward thin-film hydration/post-insertion strategy. The specific aim was not merely to produce another FA-liposomal formulation, but to provide a mechanistically validated assessment of FR-mediated targeting. We first characterized key physicochemical



Scheme 1. Schematic Illustration of Folate-conjugated Doxorubicin-loaded Liposomes (FL-DOX). DSPC: 1,2-distearoyl-sn-glycero-3-phosphocholine; Chol: cholesterol; DSPE-mPEG2000: 1,2-distearoyl-sn-glycero-3-phosphoethanolamine-N-[methoxy(polyethylene glycol)-2000]; DSPE-PEG2000-FA: folic acid–conjugated DSPE-PEG2000 (folate-PEG2000-DSPE); DOX: doxorubicin. The lipid bilayer is composed of DSPC/Chol with PEGylated DSPE, and DOX is encapsulated within the aqueous core; folate moieties on the surface enable folate receptor–mediated targeting.

parameters and examined pH-responsive release to support exposure feasibility in tumor-relevant acidic conditions. We then quantified anticancer activity in MCF-7 cells and directly tested receptor dependence using folate-competitive conditions. Finally, we performed Annexin V/PI flow cytometry to quantify apoptosis and determine whether FR-mediated uptake translates into enhanced programmed cell death. Together, these experiments address a common gap in prior studies by linking formulation performance to receptor-specific function and quantitative mechanistic endpoints.

Materials and Methods

Materials

DSPC was obtained from Lipoid GmbH (Ludwigshafen, Germany). The lipid conjugates DSPE-mPEG2000 and DSPE-PEG2000 were sourced from Avanti Polar Lipids (Alabaster, AL, USA). Cholesterol, sodium pentanesulfonate, sodium edetate, and MTT reagent were purchased from Sigma-Aldrich (St. Louis, MO, USA). Cell culture reagents such as penicillin/streptomycin, fetal bovine serum (FBS), RPMI-1640, and DMEM media were acquired from Invitrogen (Carlsbad, CA, USA). Doxorubicin hydrochloride was procured from Ebewe Pharma (Unterach, Austria). Human breast cancer MCF-7 cell lines were provided by the National Cell Bank of Iran (Pasteur Institute of Iran, Tehran). The specifics of the chemicals utilized in this study and the procedures for various experiments are available in the Supporting Information (Scheme 1).

Development of Doxorubicin-Loaded Nanoliposomes

Nanoliposomes, either drug-loaded or empty, were formulated using the conventional thin-film hydration method. Initially, lipids were combined in a molar ratio of DSPC:Chol:DSPE-mPEG2000 at 58:14:3, corresponding to approximate masses of 174 mg, 22.6 mg, and 32.4 mg, respectively, dissolved in 18 mL of chloroform. The lipid mixture was transferred to a round-bottom flask and subjected to solvent evaporation under reduced pressure using a rotary evaporator at 50 °C and 120 rpm. Residual solvent was eliminated through nitrogen gas purging. The resulting lipid film was then hydrated at 50 °C using phosphate-buffered saline (PBS, pH 7.2), either containing 8 mg of Doxorubicin for drug-loaded formulations or PBS alone for blank samples. To achieve folate-mediated targeting, 5 mg of FA-PEG2000-DSPE was post-inserted into the liposomal bilayer. Briefly, a FA-PEG2000-DSPE stock solution was prepared and added dropwise to the preformed liposomal suspension while maintaining the dispersion at 50 °C (i.e., above the lipid transition temperature). The mixture was then incubated for 30 min under continuous gentle stirring (120 rpm) to facilitate ligand insertion into the outer leaflet of the bilayer. During incubation, the suspension was intermittently vortex-mixed for 8 s every 5 min (or maintained on a low-speed orbital shaker) to ensure homogeneous mixing and prevent localized aggregation. A control formulation lacking the targeting ligand, referred to as L-Doxorubicin, was also prepared to evaluate the effect of folate conjugation. For the L-Doxorubicin preparation, the amount of mPEG2000-DSPE was increased from 31.4 mg to 47.4 mg to maintain consistent surface PEGylation. The liposomal suspensions were subsequently extruded through polycarbonate membrane filters with pore sizes of 200 nm to achieve uniform particle size distribution.

Characterization of liposomes

The average particle diameter, zeta potential, and size distribution of doxorubicin-loaded liposomes were evaluated by dynamic light scattering (DLS) using a Zetasizer Nano-ZS instrument (Malvern Instruments, UK; model ZEN3600, equipped with a 4 mW He–Ne laser at 633 nm, operated at 25 °C). Measurements were collected at a fixed scattering angle of 173° (backscatter detection). Each sample was analyzed in triplicate (three independent measurements), with each measurement comprising ≥10–15 runs as automatically set by the instrument software. The structural characteristics of liposomal vesicles were examined using transmission electron microscopy (TEM, ZEISS, Germany) and scanning electron microscopy (SEM, ZEISS, Germany). For TEM analysis, a drop of diluted liposomal dispersion was applied onto a carbon-coated copper grid, negatively stained with phosphotungstic acid, air-dried, and visualized to assess vesicle morphology and internal organization. TEM imaging was performed at an accelerating voltage of ~80 kV, and representative micrographs were acquired at ~16.700× magnification. For SEM, a thin layer of freeze-dried liposomes was prepared on a glass substrate, sputter-coated with a gold film, and observed under the microscope to evaluate surface morphology. SEM imaging was typically conducted at an accelerating voltage of ~5 kV, and representative images were captured at ~30,000× magnification (scale bar 500 nm).

Encapsulation efficiency (EE %) and loading rate (LR %) of DOX in liposomes

For this purpose, 1 ml of formulation was centrifuged (TOMY, GRX-220, Japan) at 45,000 g for 45 min at 4 °C. The amount of unentrapped DOX in the supernatant was measured by spectrophotometer at 480 nm. The concentration of free DOX in the supernatant was determined through a prepared standard curve. Then, the EE % and LR % were estimated by the following equations:

$$EE\ \% = [(\text{initial DOX} - \text{unentrapped DOX}) / \text{initial DOX}] \times 100 \quad \text{(eq. 1)}$$

Where initial DOX is the amount of drug present in 1 ml of formulation, and unentrapped DOX is the amount of the drug in the supernatant.

$$LR\ \% = (\text{entrapped DOX} / \text{weight of carrier}) \times 100 \quad \text{(eq. 2)}$$

Where entrapped DOX is the amount of drug encapsulated in the liposomes and weight of carrier is the

amount of liposomes used.

Release study

The in vitro release behavior of folic acid–modified liposomal doxorubicin (FL-DOX) was evaluated using the dialysis technique. In this experiment, 1 mL of either FL-DOX or free DOX solution was placed in a dialysis membrane (MWCO: 12 kDa; Spectra/Por® dialysis tubing, Spectrum Laboratories, USA), sealed, and immersed in 25 mL of phosphate-buffered saline (PBS) at pH 7.4 or 5.2. The samples were incubated at 37 °C with constant stirring at 120 rpm for 50 h. To maintain sink conditions, the release medium volume (25 mL) was selected to be at least 10-fold higher than the estimated saturation solubility of DOX under the tested conditions, and at each sampling time point, an equal volume of fresh pre-warmed buffer was immediately added to replace the withdrawn aliquot. This continuous medium replacement ensured that the concentration of released DOX in the external phase remained well below saturation throughout the experiment, thereby preserving sink conditions. At specific time intervals, aliquots were collected and replaced with fresh buffer to preserve sink conditions. The absorbance of the withdrawn samples was measured at λmax = 480 nm using a UV–Vis spectrophotometer, and the cumulative drug release was quantified using a standard calibration curve. The percentage release was calculated using the following expression:

$$\text{Release rate \%} = (Cs / Ct) \times 100$$

where Cs is the concentration of DOX in the collected sample at a given time, and Ct is the total DOX content initially encapsulated in the FL-DOX formulation prior to dialysis.

Cytotoxicity assay (MTT) and IC_{50} determination

The cytotoxic potential of nanoliposomal DOX formulations against MCF-7 breast cancer cells was evaluated using the MTT assay. Briefly, cells were cultured in medium supplemented with 10% fetal bovine serum (FBS), 100 µg/mL streptomycin, 100 U/mL penicillin, and 0.25 µg/mL amphotericin B, under a humidified atmosphere containing 5% CO_2 at 37 °C. Approximately 1×10^4 cells per well were seeded into 96-well plates with 200 µL of medium and incubated for 24 h to allow attachment. Following attachment, the medium was replaced with either fresh medium (negative control) or medium containing DOX formulations under the following predefined experimental conditions: F1: folate-targeted liposomal DOX (FL-DOX) in folate-depleted medium; F2: FL-DOX in normal medium supplemented with 1 mM folate (competitive condition); F3: FL-DOX in standard medium; F4: non-targeted liposomal DOX in standard medium; and F5: free DOX in standard medium. For each group (F1–F5), dose–response curves were generated by treating cells with a range of DOX-equivalent concentrations (e.g., 0.5–50 µM) for 48 h, and IC_{50} values were calculated from nonlinear regression (four-parameter logistic model). Cells were further incubated for 48 h. After treatment, 180 µL of fresh medium and 20 µL of MTT solution (5 mg/mL in PBS) were added to each well and incubated for an additional 3 h. The reaction was terminated by adding 200 µL of DMSO to dissolve the formazan crystals. The absorbance was measured at 570 nm using a microplate reader (AccuReader M965, Metertech, Taipei, Taiwan), and IC_{50} values were determined using GraphPad Prism 6 (GraphPad Software, San Diego, CA).

Cellular uptake study

The cellular internalization of the nanoliposomal formulation was evaluated in MCF-7 breast cancer cells. For this purpose, cells were seeded at a density of 3×10^5 cells per well in 24-well plates and cultured either in folate-free medium or in medium supplemented with 1 mM folic acid. After overnight incubation, receptor-bound folate was removed by washing the cells with cold PBS and acidic saline buffer (pH 3.5; 130 mM NaCl, 20 mM NaOAc). Fresh medium containing 0.07 mg/mL DOX in different formulations (FL-DOX, L-DOX, or free DOX) was then added, and the cells were incubated at 37 °C for 2 h. Non-adherent vesicles were eliminated by washing twice with PBS (pH 7.4), after which the cells were collected by centrifugation at 13,000 rpm for 5 min and lysed with 200 µL of 0.5% Triton X-100. The lysates were mixed with an equal volume of acetonitrile to precipitate proteins, centrifuged again, and the supernatant was filtered through a 0.22 µm membrane. A 20 µL aliquot of the filtrate was analyzed by HPLC, and the cellular uptake efficiency (CUE%) was calculated as:

CUE%: Amount of DOX in the cells after the incubation time/Amount DOX added in liposomal formulations introduced into the cells × 100

Apoptosis analysis by Annexin-V staining

Apoptosis induced by the FL-DOX formulation in MCF-7 cells was evaluated using the FITC Annexin V apoptosis detection kit (BioLegend Inc., San Diego, CA) following the supplier's protocol. In brief, MCF-7 cells (5×10^5 per well) were seeded into six-well plates and allowed to attach overnight at 37 °C in a 5% CO_2 incubator under folate-depleted conditions. The next day, the medium was replaced with fresh culture medium containing 2 µM of either free DOX or FL-DOX (in triplicate). After 48 h of exposure, the cells were collected, washed twice with ice-cold cell staining buffer, and resuspended in Annexin-V binding buffer at a density of 1×10^6 cells/mL. A 100 µL aliquot of this suspension was transferred into 5 mL tubes, mixed with 5 µL FITC Annexin V and 10 µL propidium iodide (PI), gently vortexed, and incubated for 15 min at room temperature in the dark. Finally, 400 µL of binding buffer was added, and the samples were analyzed by flow cytometry to determine the proportion of apoptotic cells. Flow cytometric acquisition was performed using a BD FACSCanto™ II flow cytometer (BD Biosciences, USA), and data were analyzed using FlowJo software (version X, BD/FlowJo LLC).

Statistical Analysis

Data were analyzed using SPSS v18 and are presented as mean ± SD from three independent biological experiments (n = 3), with each condition measured in technical triplicate within each experiment unless otherwise stated. For comparisons between two groups, statistical significance was assessed using an unpaired two-tailed Student's t-test (e.g., free DOX vs FL-DOX in the apoptosis assay, or other single pairwise comparisons). For experiments involving more than two groups (e.g., F1–F5 comparisons of IC_{50} values in Figure 1 and uptake/other multi-group analyses), data were analyzed using one-way ANOVA, followed by Šidák's multiple-comparisons post-hoc test to control for type I error across multiple pairwise tests. A p value of < 0.05 was considered statistically significant.

Results

Characterization of liposomes

The morphology and physicochemical characteristics of the prepared liposomes were investigated using SEM, and TEM, The SEM and TEM micrographs revealed that the vesicles were predominantly spherical in shape with a uniform distribution. Consistent with the morphological findings, the physicochemical characterization demonstrated that the mean particle size of the liposomes was 182.2 ± 12.2 nm, accompanied by a polydispersity index (PDI) of 0.24 ± 0.01, which reflects a relatively narrow size distribution. Moreover, the zeta potential was measured as −34.4 ± 4.2 mV, indicating a high degree of surface charge and favorable colloidal stability. The liposomes exhibited encapsulation and loading efficiencies of 92.4 ± 4.6% and 2.37 ± 0.3%, respectively. These combined results (Figure 2) suggest that the synthesized liposomes possessed suitable size, stability, and morphology for further biomedical applications.

Release study

The free DOX solution was completely released in less than 10 h, whereas the folic acid–conjugated liposomal formulation (FL-DOX) exhibited a markedly slower and more controlled release pattern. The in vitro release of DOX from FL-DOX was evaluated in PBS at two pH conditions (5.2 and 7.4) over 50 h. As shown in Figure 3, FL-DOX displayed a sustained release profile without an evident initial burst. At 50 h, the cumulative release reached approximately ~62% at pH 7.4 and ~90% at pH 5.2. Release profiles were compared by two-way ANOVA followed by Šidák's multiple-comparisons test; $p < 0.05$. The accelerated release under acidic conditions is consistent with pH-dependent modulation of DOX–lipid interactions and increased DOX protonation/solubility at lower pH, which can facilitate drug diffusion from the liposomal bilayer or aqueous core. Collectively, these findings indicate that FL-DOX effectively prolongs and modulates DOX release relative to free drug, supporting

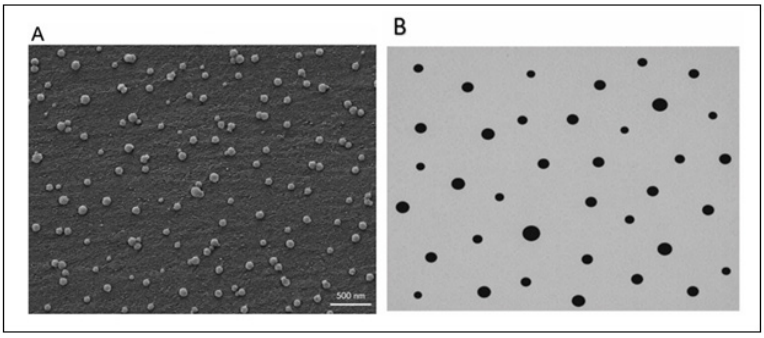


Figure 1. Morphological Visualization of PEGylated Liposomes Displaying Spheroid Vesicular Structures as Captured by SEM (A), and TEM (B).

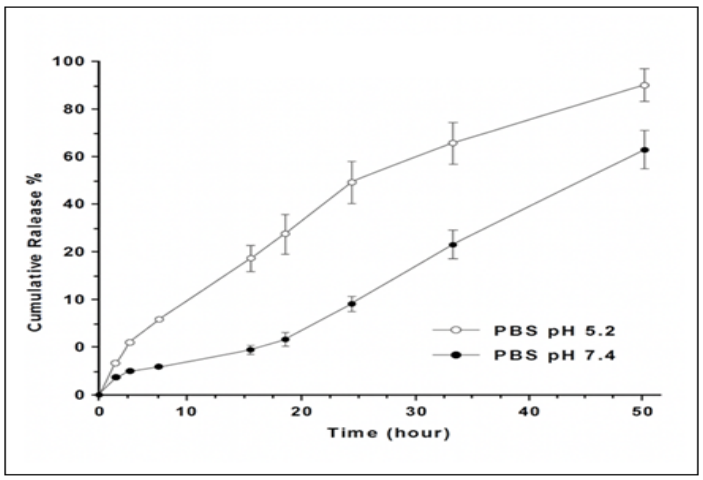


Figure 3. *In vitro* Release Profile of the Drug from Liposomes under Different pH Conditions at 37 °C Over a Period of 50 h. Data are presented as the mean ± standard deviation (SD) of three independent experiments.

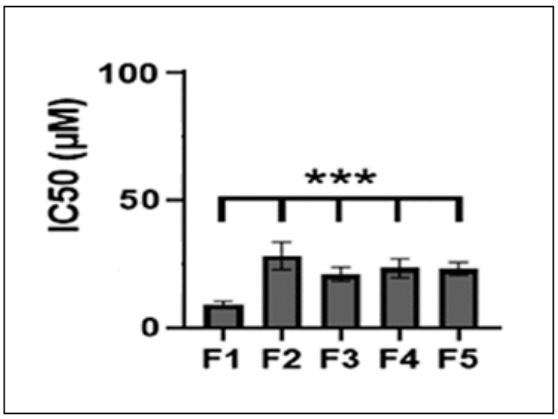


Figure 3. IC_{50} Values (μM) of Different DOX Formulations in MCF-7 Cells under Various Culture Conditions. F1: FL-DOX in folate-depleted medium; F2: FL-DOX in standard medium supplemented with 1 mM free folate (competitive condition); F3: FL-DOX in standard medium; F4: non-targeted liposomal DOX (L-DOX) in standard medium; F5: free DOX in standard medium. Data are presented as mean ± SD (n = 3). Overall group differences: p = 0.0002. (*** indicates statistical significance as shown in the figure.)

folate-targeted liposomes as a controlled drug delivery platform.

In vitro cytotoxicity assay

Following 48 hours of incubation at 37°C, the cytotoxic activity of DOX-loaded nanoliposomes was assessed in comparison with free DOX at equivalent concentrations in MCF-7 cells (Figure 1). For each tested condition (F1–F5), dose–response curves were generated and IC_{50} values were calculated by nonlinear regression analysis. The results showed that FL-DOX exhibited a markedly stronger inhibitory effect on MCF-7 cells relative to conventional DOX, particularly under folate-free culture conditions. Accordingly, the IC_{50} of FL-DOX in folate-depleted medium (F1) was approximately 7.2 μM, which was ~2.9-fold lower than that of free DOX in standard medium (F5, ~20.9 μM). However, the addition of 1 mM folate to the medium reduced this enhanced cytotoxic response. Notably, the competitive supplementation with folate increased the IC_{50} of FL-DOX (F2) to ~26.1 μM, effectively abolishing the advantage observed under folate-depleted conditions, thereby supporting a folate receptor–dependent uptake mechanism.

Cellular uptake study

To assess the involvement of folate receptors in the uptake process, the internalization of folate-modified nanoliposomes was investigated in MCF-7 cells. As illustrated in Figure 4, FL-DOX showed markedly greater uptake than L-DOX and free DOX ($p < 0.001$). This visual evidence supports efficient folate receptor–mediated internalization of the folate-conjugated liposomal system in MCF-7 cells, highlighting its potential as a targeted nanocarrier for improved cellular uptake.

Table 1. Quantification of Annexin-V/PI Staining Analysis of MCF-7 Cells after 48 h of Treatment with FL-DOX, Conventional DOX, or Control. Data are expressed as mean ± SD (n = 3).

Formulations	Vital cells % An−/PI−	Early apoptosis % An+/PI−	Late apoptosis% An+/PI+	Necrotic cells % An−/PI+
FL-DOX	51.88 ± 5.2	7.24 ± 2.1	26.39 ± 3.1	14.33 ± 1.2
Conventional DOX	61.32 ± 6.1	9.72 ± 1.5	18.97 ± 2.4	8.09 ± 1.1
Control	77.28 ± 7.0	6.45 ± 1.3	9.25 ± 1.6	5.60 ± 1.0

Apoptosis Analysis by Annexin-V Staining

As presented in Figure 5 and Table 1, flow cytometry analysis revealed that treatment with FL-DOX markedly shifted the cell population from viable cells toward apoptotic and necrotic populations compared with both conventional DOX and untreated control groups. Notably, Annexin V/PI analysis demonstrated a significantly higher late-apoptotic population (Annexin V+/PI+) in the FL-DOX group compared with conventional DOX (26.39 ± 3.1% vs 18.97 ± 2.4%; unpaired two-tailed Student's t-test, $p < 0.05$; n = 3), indicating that late apoptosis was the dominant mode of cell death following FL-DOX treatment. In contrast, conventional DOX produced a more moderate apoptotic response, whereas control cells remained largely viable with minimal apoptosis or necrosis. Overall, these findings indicate that folate-conjugated liposomal DOX enhances anticancer efficacy in MCF-7 cells by strongly promoting apoptosis particularly at the late stage supporting the advantage of receptor-targeted liposomal delivery.

Discussion

This study shows that folate-conjugated liposomal doxorubicin (FL-DOX) delivers a functionally meaningful advantage in MCF-7 cells by integrating (i) a stable nanoscale carrier (≈182 nm; PDI ≈0.24; ζ ≈ −34 mV), (ii) high DOX encapsulation (EE% ≈92%) with

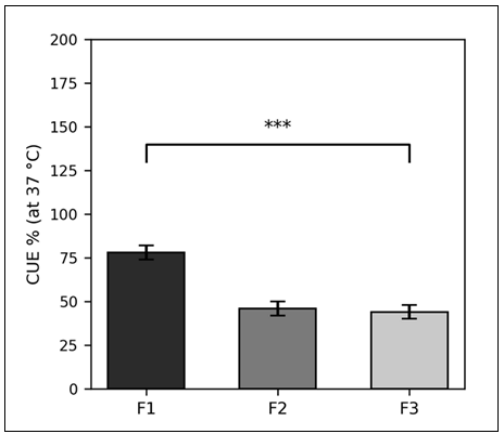


Figure 4. (A) Cellular Uptake Efficiency (CUE%) of Folate-conjugated Liposomes in MCF-7 Cells at 37 °C. Formulations include: F1, FL-DOX; F2, Free DOX; and F3, L-DOX. Data are presented as mean ± SD (n = 3; ***$p < 0.0001$).

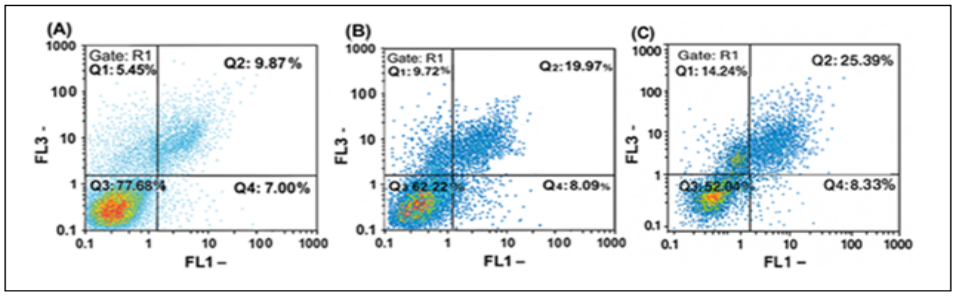


Figure 5. Annexin V–FITC/PI Flow Cytometry Analysis of Apoptosis in MCF-7 Cells after 48 h of Treatment. Representative dot plots are shown for (A) Control, (B) conventional DOX, and (C) FL-DOX. Events were first gated on R1 to exclude debris, and apoptosis was quantified using quadrant analysis with FL1 (Annexin V–FITC) on the x-axis and FL3 (PI) on the y-axis. Quadrants were defined as: Q4 (Annexin V−/PI−), viable cells; Q3 (Annexin V+/PI−), early apoptosis; Q2 (Annexin V+/PI+), late apoptosis/secondary necrosis; Q1 (Annexin V−/PI+), necrotic cells. The percentage of events in each quadrant is displayed on the plots. Identical quadrant gates (crosshairs) were applied across all treatment groups.

sustained, pH-responsive release, and (iii) receptor-linked biological effects supported by competitive folate conditions and apoptosis quantification. Morphological and physicochemical characterization using SEM, and TEM confirmed the formation of spherical vesicles with smooth surfaces and uniform size distribution [23]. In a similar study, Cintra et al., 2022 reported PEGylated folate-targeted DOX magnetoliposomes with control hydrodynamic diameters ~120 nm and a ~30% larger mean diameter for the folate-targeted DOX-loaded formulation, while DOX encapsulation efficiency remained above 90%, which is broadly comparable to our high EE (~92%) but achieved at a smaller size scale than our ~182 nm system [24]. In another study, Wang et al., 2023 reported a folate-targeted dual-loaded liposome (NIRB–DOX–FA) with size 124 nm, DOX encapsulation efficiency 71%, which places their DOX EE notably below our EE (~92%) and underscores how co-loading chemistry and remote-loading conditions can substantially affect apparent encapsulation performance [25]. To contextualize drug loading and retention, Haran et al., 1993 demonstrated that transmembrane ammonium sulfate gradients enable remote loading of anthracyclines into liposomes at very high efficiency (>90%), supporting remote-loading as a rational future optimization route when higher payload density and long-term retention are required beyond passive-loading constraints [26]. Our drug loading (≈2.37%, expressed as the w/w percentage of DOX relative to lipid) is comparable in magnitude to the low-loading liposomal DOX formulation reported by Yu et al., 2024, which achieved 2.4% w/w (DOX/HSPC) (an absolute difference of 0.03 percentage points, ≈1.25% relative), whereas the same study also reported a high-loading formulation with 12.9% w/w (DOX/HSPC) [27]. In terms of size regime for folate-based targeting, Yoo and Park, 2004 reported folate-presenting DOX nano-aggregates with an average size of ~200 nm and supported folate-receptor–mediated uptake with downstream antitumor effects in vivo, aligning conceptually with our ~182 nm carrier operating within a commonly used nanoscale window for receptor-linked delivery strategies [28]. The negative zeta potential (−34 mV) reflects strong surface charge, which contributes to colloidal stability by preventing particle aggregation [29]. This physicochemical profile is well within the optimal range for passive and active targeting in tumor tissues via the enhanced permeability and retention (EPR) effect [30]. The in vitro release profile of DOX from the liposomes revealed a significantly sustained and pH-responsive behavior [31]. Unlike free DOX, which was completely released within 10 hours, FL-DOX displayed controlled drug release over 50 hours, with accelerated release at acidic pH (5.2) compared to physiological pH (7.4) [32]. This pH-sensitive behavior is particularly advantageous for cancer therapy, as it ensures minimal drug leakage during systemic circulation (pH ~7.4) and enhanced drug release in the acidic tumor microenvironment or intracellular compartments such as endosomes and lysosomes [33]. The absence of an initial burst release further supports the stability of the liposomal structure and reduces the risk of systemic toxicity [34]. The cytotoxicity assay conducted in MCF-7 cells confirmed the superior anticancer activity of FL-DOX compared to free DOX. The enhanced cytotoxicity under folate-free culture conditions, and its attenuation upon the addition of exogenous folate, suggest that cellular uptake is mediated by folate receptor–targeted endocytosis. This receptor-mediated mechanism provides a rational basis for the observed selectivity of FL-DOX toward cancer cells overexpressing folate receptors, minimizing off-target effects in normal tissues. These findings were further corroborated by the cellular uptake studies, where confocal microscopy and quantitative uptake assays revealed significantly greater internalization of FL-DOX compared to non-conjugated liposomes (L-DOX) and free DOX [35]. Perhaps most importantly, Annexin V–based apoptosis analysis demonstrated that FL-DOX significantly increased apoptosis in MCF-7 cells, especially in the late apoptotic phase [36]. This indicates a strong pro-apoptotic effect of the targeted formulation. Compared to free DOX, which induced only moderate apoptosis, FL-DOX pushed a larger proportion of the cell population toward programmed cell death [37]. Mechanistically, the higher late-apoptotic fraction may result from folate receptor–mediated endocytosis that increases intracellular accumulation of FL-DOX and prolongs intracellular

DOX exposure. After endosomal/lysosomal trafficking, the acidic environment can accelerate DOX release, sustaining DNA-damage signaling (topoisomerase II inhibition) and oxidative/mitochondrial stress, which may amplify caspase-dependent pathways (e.g., Bax/Bcl-2 imbalance and caspase-3/9 activation) and drive cells from early apoptosis toward irreversible late apoptosis. The predominance of late apoptosis over necrosis further supports the idea that the liposomal formulation promotes a regulated and potentially less inflammatory form of cell death, which is desirable in cancer therapy [38]. Taken together, these results confirm that folate-functionalized liposomes can overcome several limitations associated with conventional DOX chemotherapy. Specifically, FL-DOX improves solubility and stability, allows for controlled and pH-responsive release, enhances targeted uptake via receptor-mediated endocytosis, and amplifies the apoptotic response in cancer cells. These advantages collectively highlight the promise of FL-DOX as a robust and efficient platform for targeted drug delivery in folate receptor–positive cancers, such as breast cancer.

Limitations

Researchers from around the world have made extensive efforts to treat diseases, particularly through in vitro cellular investigations and in vivo animal studies that provide essential experimental validation and mechanistic insight toward improved therapeutic strategies [39-42]. However, several limitations should be acknowledged in the present study. First, our evidence is currently restricted to in vitro assays and a single breast cancer cell line (MCF-7), which may limit generalizability across breast cancer subtypes with variable folate receptor expression. Second, the study did not include in vivo pharmacokinetic, biodistribution, efficacy, or safety testing; therefore, claims related to tumor targeting, EPR-mediated accumulation, or reduced cardiotoxicity remain prospective and require validation. Third, we did not perform formal stability assessments (e.g., serum stability, shelf-life at 4 °C, or leakage over time), which are important for translational feasibility. Finally, while competitive folate conditions support receptor involvement, additional receptor-specific validation (e.g., FRα expression quantification, receptor-blocking antibodies, or FRα knockdown) would further strengthen mechanistic attribution.

In Conclusion, FL-DOX integrates favorable physicochemical properties with sustained, pH-responsive release and receptor-linked functional outcomes in MCF-7 cells, culminating in enhanced cytotoxicity and a pronounced shift toward apoptosis particularly late apoptosis relative to conventional DOX. Having established superior in vitro targeting-associated performance, the next step is to evaluate FL-DOX in vivo, including pharmacokinetics and biodistribution, antitumor efficacy in orthotopic or metastatic breast cancer models, and safety endpoints with particular attention to cardiotoxicity (e.g., cardiac biomarkers and functional assessment). These studies will be essential to determine whether the mechanistic advantages observed in vitro translate into a meaningful therapeutic index improvement in vivo.

Acknowledgements

None.

Funding

The authors have no relevant financial or non-financial interests to disclose.

Competing interests

The authors have no competing interests to declare that are relevant to the content of this article.

Ethics approval

This study did not involve any original data collection or human subjects, and therefore, ethical approval was not required.

Consent

All authors have provided consent for publication.

Originality Declaration for Figures

All figures included in this manuscript are original and have been created by the authors specifically for the purposes of this study. No previously published or copyrighted images have been used. The authors confirm that all graphical elements, illustrations, and visual materials were generated from the data obtained in the course of this research or designed uniquely for this manuscript.

References

1. Alishahi F, Soudmand N, Ghasemi Goki T, Rashidoleslami TS. Optimal Pharmaceutical Management Strategies in Cancer Treatment: Novel Approaches. Asian Pacific Journal of Cancer Nursing. 2025 03 08;:20250308. https://doi.org/10.31557/apjcn.1740.20250308
2. Kanaani L, javadi I, Ebrahimi-Far M, Ebrahimi shahmabadi H, Akbarzadeh Khiyavi A, Mehrdiba T. Effects of Cisplatin-Loaded Niosomal Nanoparticleson BT-20 Human Breast Carcinoma Cells. Asian Pacific Journal of Cancer Prevention. 2017 02;18(2). https://doi.org/10.22034/APJCP.2017.18.2.365
3. Saberian E, Jenča A, Petrášová A, Zare-Zardini H, Ebrahimifar M. Application of Scaffold-Based Drug Delivery in Oral Cancer Treatment: A Novel Approach. Pharmaceutics. 2024 06 14;16(6):802. https://doi.org/10.3390/pharmaceutics16060802
4. Ghanbarikondori P, Aliakbari RBS, Saberian E, Jenča A, Petrášová A, Jenčová J, Khayavi AA. Enhancing Cisplatin Delivery via Liposomal Nanoparticles for Oral Cancer Treatment. Indian Journal of Clinical Biochemistry. 2025 04;40(2):211-217. https://doi.org/10.1007/s12291-024-01239-3
5. Cheng X, Xie Q, Sun Y. Advances in nanomaterial-based targeted drug delivery systems. Frontiers in Bioengineering and Biotechnology. 2023 04 13;11:1177151. https://doi.org/10.3389/fbioe.2023.1177151
6. Khakbiz M, Chagami M, Sheibani S, Amiri E, Moazzeni S, Shakibania S, Hou Y, Lee K. Enhancement of corrosion,

biocompatibility and drug delivery properties of nitinol implants surface by Al-Zn-LDH nanohybrids. Colloids and Surfaces A: Physicochemical and Engineering Aspects. 2025 01;704:135524. https://doi.org/10.1016/j.colsurfa.2024.135524
7. Bardajee GR, Shafiei N, Rouhi M, Mahmoodian H. Inverse Miniemulsion Polymerization of Dual-Responsive Single-Network Alg-PDMAEMA Nanogels Colon-Targeted DOX Delivery. Journal of Cluster Science. 2025 07 11;36(4):149. https://doi.org/10.1007/s10876-025-02865-4
8. Amiri F, Alishahi F, Mohammadifar G, Izadidehkordi S, Charmduzi F, Dialameh F, Khiyavi AA. Enhanced Anticancer Efficacy of Selenium Nanoparticles Encapsulated in Niosomes: A Novel Therapeutic Strategy. Indian Journal of Clinical Biochemistry. 2025 04 23;. https://doi.org/10.1007/s12291-025-01321-4
9. Sadeghzadeh M, Farhadi S, Rahmati H, Darabi Z, Ehsani F, Basirat M, Amini M. Probiotic-Derived Extracellular Vesicles as Immunomodulatory Agents in Autoimmune Disease Management. Nanomedicine Research Journal. 2025 Dec;10(4). https://doi.org/10.22034/nmrj.2025.04.006
10. Jafari M, Ansari Damavandi S, Charmduzi F. Transformation of acute lymphoblastic leukemia with a precursor B-cell immunophenotype to burkitt's lymphoma: A case report. Caspian Journal of Internal Medicine. 2023 09;14(4). https://doi.org/10.22088/cjim.14.4.760
11. Mahmoudian F, Gheshlagh SR, Hemati M, Farhadi S, Eslami M. The influence of microbiota on the efficacy and toxicity of immunotherapy in cancer treatment. Molecular Biology Reports. 2025 Dec;52(1):86. https://doi.org/10.1007/s11033-024-10188-2
12. Rahiman N. Updates and current states on liposomal vehicles for tumor targeting: precision therapy in the spotlight. Cancer Nanotechnology. 2025 Dec;16(1):12. https://doi.org/10.1186/s12645-025-00314-5
13. Kalra J, Baker J, Sun X, Kyle A, Minchinton A, Bally MB. Accumulation of liposomes in metastatic tumor sites is not necessary for anti-cancer drug efficacy. Journal of Translational Medicine. 2024 07 03;22(1):621. https://doi.org/10.1186/s12967-024-05428-9
14. Cheung A, Bax HJ, Josephs DH, Ilieva KM, Pellizzari G, Opzoomer J, Bloomfield J, et al. Targeting folate receptor alpha for cancer treatment. Oncotarget. 2016 08 09;7(32):52553-52574. https://doi.org/10.18632/oncotarget.9651
15. Gonzalez T, Muminovic M, Nano O, Vulfovich M. Folate Receptor Alpha A Novel Approach to Cancer Therapy. International Journal of Molecular Sciences. 2024 01 15;25(2):1046. https://doi.org/10.3390/ijms25021046
16. Yi Y. Folate Receptor-Targeted Diagnostics and Therapeutics for Inflammatory Diseases. Immune Network. 2016;16(6):337. https://doi.org/10.4110/in.2016.16.6.337
17. Christowitz C, Davis T, Isaacs A, Van Niekerk G, Hattingh S, Engelbrecht A. Mechanisms of doxorubicin-induced drug resistance and drug resistant tumour growth in a murine breast tumour model. BMC Cancer. 2019 Dec;19(1):757. https://doi.org/10.1186/s12885-019-5939-z
18. Rivankar S. An overview of doxorubicin formulations in cancer therapy. Journal of Cancer Research and Therapeutics. 2014;10(4):853. https://doi.org/10.4103/0973-1482.139267
19. Bhadran A, Polara H, Babanyinah GK, Baburaj S, Stefan MC. Advances in Doxorubicin Chemotherapy: Emerging Polymeric Nanocarriers for Drug Loading and Delivery. Cancers. 2025 07 10;17(14):2303. https://doi.org/10.3390/cancers17142303
20. Zhang B, Zhang Y, Dang W, Xing B, Yu C, Guo P, Pi J, et al. The anti-tumor and renoprotection study of E-[c(RGDfK)2]/folic acid co-modified nanostructured lipid carrier loaded with doxorubicin hydrochloride/salvianolic acid A. Journal of Nanobiotechnology. 2022 09 24;20(1):425. https://doi.org/10.1186/s12951-022-01628-x
21. Mohseni M, Faghihi R, Haghighatafshar M, Entezarmahdi SM. Effects of the attenuation correction and reconstruction method parameters on conventional cardiac dynamic SPECT. Medicine. 2018 09;97(39):e12239. https://doi.org/10.1097/MD.0000000000012239
22. Jamalpour H, Feiz M, Jamalpour Z, Darvishian Kermanshahi G, Yari F. Rescripting Psychic Pathologies: CRISPR-Cas9's Biochemical Reconfiguration of Mental Health in Cultural and Bioethical Contexts of Post-2000 Speculative Fiction and Autobiographical Narratives. Cultural Conflict and Integration. 2025 09 10;2(2). https://doi.org/10.55121/cci.v2i2.532
23. Dave V, Gupta A, Singh P, Gupta C, Sadhu V, Reddy KR. Synthesis and characterization of celecoxib loaded PEGylated liposome nanoparticles for biomedical applications. Nano-Structures & Nano-Objects. 2019 04;18:100288. https://doi.org/10.1016/j.nanoso.2019.100288
24. Cintra ER, Hayasaki TG, Sousa-Junior AA, Silva ACG, Valadares MC, Bakuzis AF, Mendanha SA, Lima EM. Folate-Targeted PEGylated Magnetoliposomes for Hyperthermia-Mediated Controlled Release of Doxorubicin. Frontiers in Pharmacology. 2022 03 21;13:854430. https://doi.org/10.3389/fphar.2022.854430
25. Wang L, Evans JC, Ahmed L, Allen C. Folate receptor targeted nanoparticles containing niraparib and doxorubicin as a potential candidate for the treatment of high grade serous ovarian cancer. Scientific Reports. 2023 02 24;13(1):3226. https://doi.org/10.1038/s41598-023-28424-3
26. Haran G, Cohen R, Bar LK, Barenholz Y. Transmembrane ammonium sulfate gradients in liposomes produce efficient and stable entrapment of amphipathic weak bases. Biochimica et Biophysica Acta (BBA) - Biomembranes. 1993 09;1151(2):201-215. https://doi.org/10.1016/0005-2736(93)90105-9
27. Yu Y, Wu E, Lin S, Chu Y, Yang Y, Pan F, Ding T, et al. Reexamining the effects of drug loading on the in vivo performance of PEGylated liposomal doxorubicin. Acta Pharmacologica Sinica. 2024 03;45(3):646-659. https://doi.org/10.1038/s41401-023-01169-5
28. Yoo HS, Park TG. Folate-receptor-targeted delivery of doxorubicin nano-aggregates stabilized by doxorubicin–PEG–folate conjugate. Journal of Controlled Release. 2004 Nov;100(2):247-256. https://doi.org/10.1016/j.jconrel.2004.08.017
29. Saraswat AL, Maher TJ. Development and optimization of stealth liposomal system for enhanced in vitro cytotoxic effect of quercetin. Journal of Drug Delivery Science and Technology. 2020 02;55:101477. https://doi.org/10.1016/j.jddst.2019.101477
30. Dinakar YH, Karole A, Parvez S, Jain V, Mudavath SL. Folate receptor targeted NIR cleavable liposomal delivery system augment penetration and therapeutic efficacy in breast cancer. Biochimica et Biophysica Acta (BBA) - General Subjects. 2023 09;1867(9):130396. https://doi.org/10.1016/j.bbagen.2023.130396
31. Oliveira Silva J, Fernandes R, Oda C, Ferreira T, Botelho A, Melo M. Folate-coated, long-circulating and pH-sensitive liposomes enhance doxorubicin antitumor effect in a breast cancer animal model. Biomedicine & Pharmacotherapy. 2019;. https://doi.org/10.1016/j.biopha.2019.109323
32. Chen Y, Cheng Y, Zhao P, Zhang S, Li M, He C. Co-delivery of doxorubicin and imatinib by pH sensitive cleavable PEGylated nanoliposomes with folate-mediated

targeting to overcome multidrug resistance. International Journal of Pharmaceutics. 2018;. https://doi.org/10.1016/j.ijpharm.2018.03.024
33. Paliwal S, Paliwal R, Pal H, Saxena A, Sharma P, Gupta P. Estrogen-anchored pH-sensitive liposomes as nanomodule designed for site-specific delivery of doxorubicin in breast cancer therapy. Molecular Pharmaceutics. 2012;9(1). https://doi.org/10.1021/mp200439z
34. Mamasheva E, O'Donnell C, Bandekar A, Sofou S. Heterogeneous liposome membranes with pH-triggered permeability enhance the in vitro antitumor activity of folate-receptor targeted liposomal doxorubicin. Molecular Pharmaceutics. 2011;8(6). https://doi.org/10.1021/mp200079y
35. Zheng M, Gong P, Zheng C, Zhao P, Luo Z, Cai L. Lipid-Polymer Nanoparticles for Folate-Receptor Targeting Delivery of Doxorubicin. Journal of Nanoscience and Nanotechnology. 2015;15(7). https://doi.org/10.1166/JNN.2015.9604
36. Guo F, Jiao Y, Hong W, Zhou K, Ji X, Yuan H. Star polyester-based folate acid-targeting nanoparticles for doxorubicin and curcumin co-delivery to combat multidrug-resistant breast cancer. Drug Delivery. 2021;. https://doi.org/10.1080/10717544.2021.1960926
37. Cé R, Couto G, Pacheco B, Dallemole D, Paschoal J, Guterres S. Folic acid-doxorubicin polymeric nanocapsules: a promising formulation for the treatment of triple-negative breast cancer. European Journal of Pharmaceutical Sciences. 2021; https://doi.org/10.1016/j.ejps.2021.105943
38. Angelopoulou A, Kolokithas-Ntoukas A, Fytas C, Acid-Functionalized AK. Condensed Magnetic Nanoparticles for Targeted Delivery of Doxorubicin to Tumor Cancer Cells Overexpressing the Folate Receptor. ACS Omega. 2019;. https://doi.org/10.1021/acsomega.9b03594
39. Jafarkhani S, Amiri E, Moazzeni S, Zohoorian-Abootorabi T, Eftekhary M, Aminnezhad S. Exploring the effects of micro-nano surface topography on MG63 osteoblast-like cell responses: An in vitro study. Colloids and Surfaces A: Physicochemical and Engineering Aspects. 2023;. https://doi.org/10.1016/j.colsurfa.2023.131872
40. Moghaddam Z, Mokhtari-Dizaji M, Movahedin M. Effect of acoustic cavitation on mouse spermatogonial stem cells: colonization and viability. Journal of Ultrasound in Medicine. 2021;40(5). https://doi.org/10.1002/jum.15476
41. Mendieta M, Bandegi M, Biltekin E, Akay Y, Ozpolat B, Akay M. MiR 329/449 suppresses cell proliferation, migration and synergistically sensitizes GBM to TMZ by inhibiting Src/FAK, NF-κB, and cyclin D1 activity. International Journal of Molecular Sciences. 2025;. https://doi.org/10.3390/ijms26125533
42. Ahim S, Bandegi M, Ghanbarzadeh E, Heidarzadehpilehrood R. Non-coding RNAs in neurodegeneration: an axis-based, evidence-tiered mechanistic synthesis. Metabolism Open. 2026;06;30. https://doi.org/10.1016/j.metop.2026.100458

This work is licensed under a Creative Commons Attribution-Non Commercial 4.0 International License.